

Improving the sound absorbing performance of hemp fibrous material

Abstract

Compared to the traditional synthetic fibrous materials, natural fibres represent a more sustainable solution to be used in noise control engineering and acoustic treatments. However, while synthetic fibres have been studied for almost fifty years, the knowledge of natural fibres is still limited and needs to be improved. Natural fibres are affected by a large variability of the physical properties, which consequently causes a great uncertainty in numerical modelling and difficulties during the design process of acoustics treatments. This study highlights the possibility to enhance the acoustic performance of hemp fibrous materials through the manufacturing process, investigating how each treatments affects the material physical characteristics and its sound absorption coefficient. Moreover, a simplified model to evaluate the acoustic performance of hemp fibrous materials as a function of their density is proposed, in order to provide a practical tool to investigate and compare different solutions. The physical parameters numerically evaluated for a varying compression rate have been compared with the experimental results, measured at each stage of the production process on samples of several densities. The global reliability of the proposed approach is finally investigated by comparing the experimental sound absorption for normal incidence with the results obtained from the Johnson-Champoux-Allard model, implemented with the numerically evaluated material physical parameters.

Keywords: sustainability, hemp-fibrous material, sound absorption coefficient, material characterisation, JCA model

1. Introduction

As sound insulation and noise control became a primary concern in many industrial fields, several porous and fibrous materials have been developed, by using polymers and petroleum-based products. However, thanks to the global effort in pursuing the reduction of energy consumption, aiming to a more sustainable development, which will preserve resources for future generations, in the last decade sustainable material have been increasingly studied also within the field of noise control engineering. The sustainability of a material is generally considered in terms of resources usage, environmental impact, human health, and social equity. Moreover, the production process should require the least amount of energy consumption – green energy is preferable to non-renewable resources – and have the minimum manufacturing waste, or provide second life options for the wasted products. Besides, the traditional petroleum-based materials such as melamine and polyurethane foams, or polyester fibres, there are materials which, even though they are derived from natural or recycled products, need to be sealed since may contain substances impacting on human health if get in contact with the skin or are inhaled. On the other hand natural materials such as wood, coconut, kenaf and hemp fibres, other being obtained from renewable resources by means of a manufacturing process with a reduced impact

17 on the environment, are also harmless for human health, since do not contain toxic substances
18 [1, 2]. For these reasons, compared the traditional materials employed in building construction
19 to improve the thermal and acoustic performances, natural fibres represent an eco-friendly sus-
20 tainable solution. Hemp-based materials have been widely used in building construction, either
21 in fibre-reinforced concrete, or other bio-composites, or as thermal insulation material [3] and
22 again as teharmo-mechanical reinforcement in gypsum plaster panels [4]. Moreover, recent stud-
23 ies have shown that natural fibres can also be employed for both sound insulation and sound
24 absorption applications [5, 6, 7]. In the literature several acoustical model to investigate differ-
25 ent kinds fibrous materials can be found. The most widely used empirical model for mineral
26 and glass wool is probably the one developed by Delany and Bazley [8]. This model was later
27 modified by Miki [9], providing alternative expressions for the complex wavenumber and the
28 characteristic impedance. Other models have also been developed in order to investigate differ-
29 ent fibrous, porous or granular materials, like, for example, the widely used Johnson-Champoux-
30 Allard equivalent fluid model [10, 11] which takes into account both the visco-inertial dissipative
31 effect and the thermal dissipative effect inside the material, or the alternative model propped by
32 Lafarge [12], or again the model specifically developed for polyester fibres by Garai and Pompoli
33 [13]. While conventional fibrous materials have been thoroughly investigated and the physical
34 parameters which affects their acoustic performance are well known, the knowledge of the phys-
35 ical characteristics of natural fibrous materials is still limited, as it is regarding the influence
36 these might have on their acoustic performance. Moreover, the manufacturing process of natural
37 fibres is not optimised in order to increase their acoustic performance; being generally produced
38 in a lower amount compared to synthetic fibres, either in small enterprises, or sometimes even in
39 artisan workshops, they are characterised by a significant variability of the fibres dimension and
40 the other physical properties. The fact that the fibres' diameter distribution can not be arbitrary
41 controlled like in the production process of synthetic fibres represents an issue for the evaluation
42 of their acoustic performance, since all the acoustic models have been generally developed for
43 homogeneous fibrous materials with a constant diameter [14, 15].

44 In this study an experimenatal investigation on the variety *Liptko* of the plant species *Cannabis*
45 *Sativa* has been performed. Only few studies, recently published, on the characterisation of hemp
46 fibres can be found in the literature [16, 17]. The aim of this work is to investigate some aspects
47 which, to the authors best knowledge, have never been analysed before for this kind of fibrous
48 material, even though they may have a significant influence on its acoustic behaviour. As it was
49 noticed, rough hemp-fibrous materials exhibited a relevantly lower sound absorption compared
50 to synthetic materials, such as polyester fibres. Therefore, the influence that the different stages
51 of the manufacturing process have on the physical characteristics and how those affect the ma-
52 terial's sound absorption have been analysed, in order to define the mechanical and chemical
53 treatments that optimises the acoustic performance of such sustainable eco-friendly and fibrous
54 material, which may be largely used in building construction. Furthermore, a simplified ap-
55 proach to characterised the physical parameters of hemp-fibrous material, which are required to
56 evaluate their sound absorption coefficient, based on the knowledge of the fibres' radius and the
57 material's apparent density, is proposed. The methodology makes use of a fluid dynamic model
58 [18] to determine, from the experimental air flow resistivity, an effective radius of the equivalent
59 homogeneous fibrous-material. Moreover, from the air flow resistivity and the absorption coef-
60 ficient for normal incidence of the hemp fibrous material, measured at a given compression rate
61 of the fibrous material, it is possible to define all the macroscopic parameters required as input
62 data in the Johnson-Champoux-Allard (JCA) model. From this initial set of parameters, defined
63 for a given density and thickness, the proposed methodology, based on Castagnède's model [19],

64 allows to to investigate the material's physical parameters and consequently the sound absorption
65 coefficient for any compression rate. The method was validated by comparing the numerical re-
66 sults evaluated at four different stages of the manufacturing process with the experimental data.
67 In the next section the investigated material is introduced and different stages of the manufac-
68 turing process are described. In section 3 the basics of Johnson-Champoux-Allard model are
69 summarised. The proposed methodology to characterised the material's physical parameter is
70 given in details in section 4, while the main results are validated and discussed in section 5.

71 2. Material and manufacturing process description

72 Hemp is a herbaceous plant of the species *Cannabis Sativa L.* The most inner part of hemp
73 stems, often referred as the pith, is surrounded by woody-fibres known as hurds or shives. The
74 most outer layer, which encloses the hurds, is made of bast fibres. By processing hemp stems two
75 different products are usually obtained: namely the hurds and the fibres. While the first is used for
76 composites productions, such as hempcrete or hemplime, the fibres represent the most valuable
77 part of the stem and are used both in reinforced concrete, and especially to produce thermal
78 insulating materials. On the other hand, this fibres do not provide an acoustic performance which
79 can make them competitive with the more traditional fibrous materials. In other to increase the
80 sound absorbing performance of this sustainable material, this study focused on the assessment
81 of the influence on the acoustic properties of different manufacturing processes the hemp fibres
82 may be subject to. The loose fibres obtained from *Cannabis Sativa L.* underwent subsequently
83 thought four different treatments:

- 84 1. **01.CAR – Carding:** this mechanical process is made in order to break down and untangle
85 long fibres, to remove the remaining traces of dirt and the shortest fibres [20].
- 86 2. **02.NaOH – NaOH alkaline treatment (5%/h):** this chemical procedure removes non-
87 cellulose compositions in hemp bast and facilitates the fibrils extraction, improving the
88 fibres quality [21, 22].
- 89 3. **03.WTC – Wide tooth combing:** a wide tooth comb is used in order to direct the fibres
90 along a certain direction, reduce the amount of short fibres and eliminate the remaining
91 non-cellulose components extracted by the alkaline treatment.
- 92 4. **04.FTC – fine tooth combing:** this last mechanical process is a further refinement of the
93 previous step 03.WTC, in this case a fine tooth comb is used instead of the wide tooth one.

94 After each step of the manufacturing process, samples of hemp fibres have been sputter-coated
95 in gold in order to be analysed with a scanning electronic microscope SEM. From the images
96 reported in Figure 1, obtained by using a SEM ZEISS EVO M15 with accelerating voltage of
97 15 kV, one can see how each stages of the manufacturing process drastically changes the fibres
98 diameters. A significant reduction of the mean diameter of the fibres is shown from step 01.CAR
99 to step 04.FTC, moreover, the amount of coarser fibres decreases. Even though a large dispersion
100 is still found in the diametres distribution, thus the determination of an effective, or weighted-
101 averaged, radius [23] is not trivial and certainly affected by a significant uncertainty. The effective
102 radius can be used to compute the material physical parameters of a fibrous materials, however,
103 a highly uncertain esteem would provide inaccurate results. For these reason, in the proposed
104 methodology a fluid dynamic effective radius determined, as described in the section 4, from the
105 experimental air flow resistivity was used, rather than an effective radius esteem based on SEM
106 images. In Table 1 are reported both the minimum and maximum radius and the effective fluid
107 dynamic radius evaluated for each material.

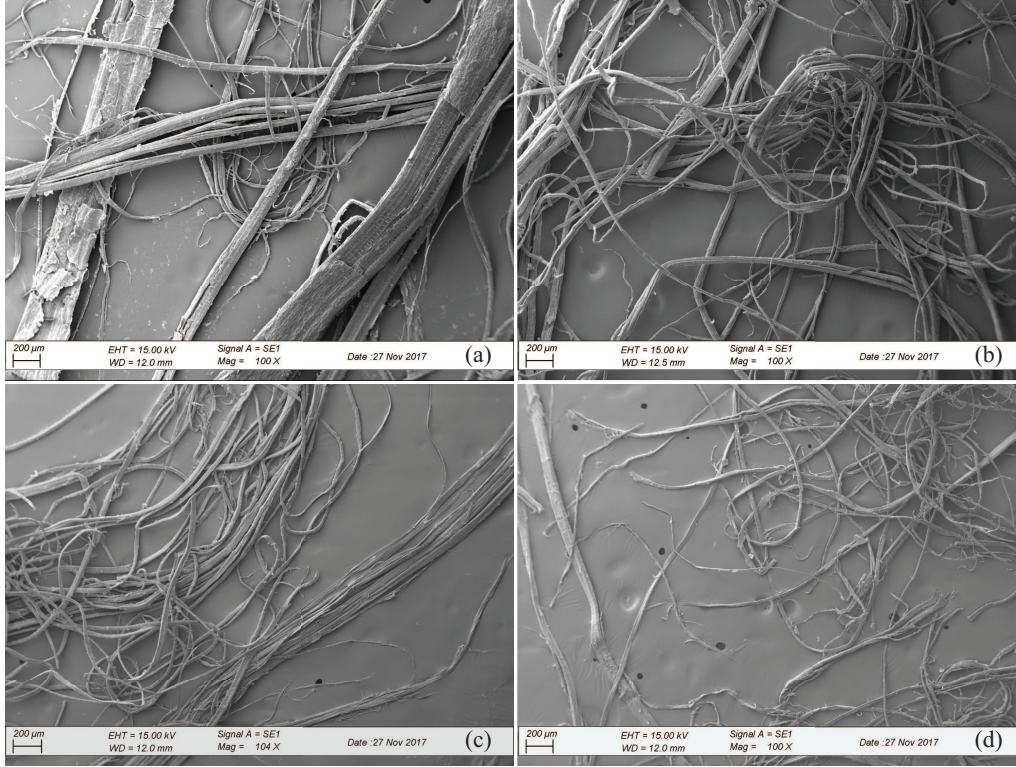


Figure 1: SEM images of hemp fibres: a) hemp fibres after carding process: 01.CAR; b) hemp fibres after alkaline treatment: 02.NaOH; c) hemp fibres after wide tooth combing: 03.WTC; d) hemp fibres after fine tooth combing: 04.FTC.

108 3. Acoustical model for sound absorption

109 For a great variety of fibrous and porous materials excited by an incident acoustic wave, it is
 110 possible to assume their solid frame to be rigid, either due to the high value of the elastic modulus,
 111 or the high density, or again because of special test conditions. These media can be described as
 112 equivalent fluids, characterised by an effective density ρ and an effective bulk modulus K . The
 113 well known Johnson-Champoux-Allard (JCA) equivalent fluid model [10, 11] is based on five
 114 macroscopic parameters:

- 115 • *airflow resistivity* - σ [Ns/s^4]: it is the resistance of the material to an airflow passing
 116 through it. The airflow resistivity is determined as:

$$117 \quad \sigma = \frac{\Delta p}{h v_{airflow}} \quad (1)$$

118 where Δp is the pressure drop across the medium while $v_{airflow}$ is the airflow rate passing
 119 through the medium of thickness h .

120

Table 1: Minimum and maximum radius of the hemp fibres determined from SEM images at each stage of the manufacturing process and equivalent effective radius based on a fluid dynamic analysis.

	01.CAR	02.NaOH	03.WTC	04.FTC
$r_{min,SEM}$ [μm]	5.33	5.86	4.56	2.39
$r_{max,SEM}$ [μm]	176.55	52.5	50.05	56.65
$r_{effect,FD}$ [μm]	27.31	29.30	22.74	18.41

- 121 • *open porosity* - ϕ [-]: it represents the fractional amount of air volume within the inter-
 122 connected pores in the medium. It can be evaluated as the ration between the air volume
 123 V_{fluid} and the total volume V_{total} of the investigated material.

$$124 \quad \phi = \frac{V_{fluid}}{V_{tot}} \quad (2)$$

- 125 • *tortuosity* - α_∞ [-]: this dimensionless quantity evaluate the sinuous fluid paths through
 126 the material. It is defined as:

$$127 \quad \alpha_\infty = \frac{\frac{1}{V} \int_V v^2 dV}{\left| \frac{1}{V} \int_V \vec{v} dV \right|^2} \quad (3)$$

128 where v is the microscopic velocity of an inviscid fluid within the pores and V is the
 129 equivalent homogeneous fluid volume.

- 130 • *viscous and thermal characteristic lengths* - Λ, Λ' [μm]: this two quantities describe the
 131 viscous forces and the thermal exchanges between the solid frame and the saturated fluid
 132 contained in it. Their influence is significant at high frequencies. They are defined as:

$$133 \quad \Lambda = 2 \frac{\int_V |v(r)|^2 dV}{\int_S |v(r)|^2 dS} \quad (4)$$

$$135 \quad \Lambda' = 2 \frac{\int_V dV}{\int_S dS} \quad (5)$$

136 where V is the volume of the fluid contained within the pores and S is the interface surface
 137 between the solid frame and the fluid.

138 The effective density ρ of the porous material, which is associated to the inertial and viscous
 139 forces, can be determined as:

$$140 \quad \rho = \frac{\alpha_\infty \rho_0}{\phi} + \frac{\sigma}{j\omega} \sqrt{1 + \frac{4j\alpha_\infty^2 \eta \rho_0 \omega}{\sigma^2 \Lambda^2 \phi^2}} \quad (6)$$

141 where ρ_0 is the air density and η its viscosity. The effective bulk modulus K takes into account
 142 the thermal exchanges between the frame and fluid. It can be determined using the formulation:

$$143 \quad K = \frac{\gamma P_0}{\phi} \left[\gamma - (\gamma - 1) \left(1 + \frac{8\eta}{j\rho_0 \omega N_{Pr} \Lambda'^2} \sqrt{1 + \frac{j\rho_0 \omega N_{Pr} \Lambda'^2}{16\eta}} \right)^{-1} \right] \quad (7)$$

5

144 being N_{Pr} the Prandtl number, γ the specific heat ratio and P_0 the static pressure. From the
 145 equivalent density and the equivalent bulk modulus, both complex quantities, the characteristic
 146 impedance Z_c and the complex wavenumber k_c can be computed:

$$147 \quad Z_c = \sqrt{\rho K} \quad (8)$$

$$148 \quad k_c = \omega \sqrt{\frac{\rho}{K}} \quad (9)$$

149 Considering a porous material of thickness h placed on a rigid reflecting boundary the surface
 150 impedance for normal incidence Z_s can be determined as:

$$151 \quad Z_s = -jZ_c \cot(k_c h) \quad (10)$$

152 the normal incidence sound absorption coefficient α_n is finally evaluate as:

$$153 \quad \alpha_n = \frac{4\text{Re}\left\{\frac{Z_s}{\rho_0 c_0}\right\}}{\left|\frac{Z_s}{\rho_0 c_0}\right|^2 + 2\text{Re}\left\{\frac{Z_s}{\rho_0 c_0}\right\} + 1} \quad (11)$$

154 where c_0 represent the speed of sound in air.

155 4. Proposed methodology

156 4.1. Single density material characterisation

157 In order to determine all the five physical parameters of the hemp fibrous material at each
 158 stage of the manufacturing process, required as input data in the JCA model, an approach based
 159 on an equivalent effective radius as been used. Considering a fibrous material with homogeneous
 160 fibres, the physical properties can be determined from the fibres radius r . Based on a fluid
 161 dynamic analysis, Tarnow [24] derived a relationship between the constant fibres radius r and
 162 the air flow resistivity σ , considering randomly distributed fibres and an air flow perpendicular
 163 to their axes:

$$164 \quad \sigma = \frac{4\pi\eta}{b^2 \left[0.64 \ln\left(\frac{b^2}{\pi r^2}\right) - 0.737 + \frac{\pi r^2}{b^2} \right]} \quad (12)$$

165 the coefficient b can be computed from the ratio between the fibres density ρ_g and the density of
 166 the fibrous material ρ_w as [18]:

$$167 \quad b = r \sqrt{\pi \frac{\rho_g}{\rho_w}} \quad (13)$$

168 Therefore, being the air flow resistivity an easily measurable quantity, the effective radius r
 169 of an equivalent homogeneous material with single diameter fibres can be computed using a
 170 simple minimisation algorithm based on Eq. (12). To this purpose, samples of loose hemp
 171 fibres, resulting from each manufacturing process described in the section 2, were tested in the
 172 acoustic laboratories of the University of Ferrara. For each sample the air flow resistivity σ was
 173 measured by means of the alternate flow method, as described in the EN 29053:1993 standard
 174 [25]; moreover the normal incidence sound absorption coefficient α_n was measured by using
 175 a well-established transfer function method in an impedance tube, according to the ISO 10534-
 176 2:1998 [26]. The cylindrical samples were prepared by compressing the loose hemp fibres into



Figure 2: Investigated hemp fibres: a) loose hemp fibres; b) a fibrous material sample is created within the test rig; c) metallic mesh used to restrain the fibres in the sample holder.

178 the sample holder, of each measurement test rig, as shown in Figure 2. A coarse metallic mesh
 179 was used to restrain the fibres when compressed in order to obtain samples with a constant
 180 density and also to prevent any leakage around the edge. For each processing stage three different
 181 measurements have been performed, each time the sample was removed and reinserted in the
 182 test rig. The fibrous material porosity ϕ was computed from the mass of loose hemp fibres, the
 183 volume of the sample holder it was contained within and the density of the fibres, according to
 184 the relationship:

$$185 \quad \phi = 1 - \frac{\rho_w}{\rho_g} \quad (14)$$

186 where ρ_w represent the density of the fibrous material and ρ_g the density of the fibres, which was
 187 estimated from the literature: $\rho_g = 1300 \text{ kg/m}^3$. The tortuosity can be evaluated as a function of
 188 the material porosity as [27]:

$$189 \quad \alpha_\infty = \left(\frac{1}{\phi}\right)^{0.7659} \quad (15)$$

190 It is possible to estimate the thermal characteristic length Λ' as a function of the mean square
 191 radius of the hemp fibres r [19], evaluated from the measured air flow resistivity using Eq. 12 as:

$$192 \quad \Lambda' = b - r \quad (16)$$

193 By knowing these four physical parameters, the viscous characteristic length Λ can be finally
 194 evaluated from the measured absorption coefficient α_n by using a well established inversion
 195 method [28].

196 4.2. Material characterisation varying the compression rate

197 The analysis was further extend investigating the possibility to compute the physical param-
 198 eters of hemp fibrous material with a arbitrary compression rate. For example the formulations
 199 developed by Castagnède et al. [19], either for 1D and 2D compression, allow to evaluate all the
 200 five physical parameters for any compression rate $n = \rho_{w,(n)}/\rho_{w,(0)}$ by knowing the material char-
 201 acteristics for a given density $\rho_{w,(0)}$ and thickness $h_{(0)}$. The great advantage of this approach is

202 certainly represented by the fact that it can be easily applied in practical contexts, requiring few
 203 simple experimental measurements. However, it should be mentioned that the linear relation-
 204 ships, developed for 1D compression, have been validated only for material with high internal
 205 porosity within the range $\phi = 0.944 \div 0.995$. In fact, it has been proved [29, 30] that Castagnède
 206 formulas for 1D compression provide reliable results when a small compression rate and highly
 207 porous materials are considered, although it may inaccurate to investigate high density materi-
 208 als. Moreover, this approach does not take into account the variation of the fibres orientation
 209 due to the compression, which has been prove to have a significant influence on the physical
 210 properties of the material [30]. Nevertheless, Castagnède model due to its simplicity and
 211 straightforward applicability represents a good starting point to define an empirical tool to be
 212 used in order to characterise hemp fibres, which have never been systematically analysed before
 213 from an acoustic point of view. To this purpose, the linear relationships associated to mono-
 214 axial 1D compression, to define the physical parameters of the JCA model, have been used, even
 215 though a correction coefficient has been introduced as exponential of the compression rate in the
 216 formulation of the air flow resistivity. Instead of the linear relationship proposed by Castagnède
 217 for 1D compression, the compression rate n is raised to the power of $A = 2.1337$. Such
 218 coefficient was determined though a least square minimisation of the percentage error between
 219 the computed air flow resistivity and the experimental data, measured on samples of five different
 220 thickness for each investigated material. Indicating with the subscript (0) the initial set of phys-
 221 ical parameters, determined as described in the previous section, and with the subscript (n) the
 222 material properties evaluated for any given compression rate n , Castagnède relationships have be
 223 reformulated as:

$$224 \quad \sigma_{(n)} = n^A \sigma_{(0)} \quad (17)$$

$$225 \quad \alpha_{\infty,(n)} = 1 - n (1 - \alpha_{\infty,(0)}) \quad (18)$$

$$226 \quad \Lambda_{(n)} = \frac{\Lambda_{(0)}}{n^{1/2}} + r \left(\frac{1}{n^{1/2}} - 1 \right) \quad (19)$$

$$227 \quad \Lambda'_{(n)} = \frac{\Lambda'_{(0)}}{n^{1/2}} + r \left(\frac{1}{n^{1/2}} - 1 \right) \quad (20)$$

231 The material's porosity was determined as ratio between the material density and the fibres den-
 232 sity, as provided in Eq. (14). The hemp fibrous material was characterised for any compression
 233 rate within the range $n = 0.5 \div 2$, starting from the physical parameters determined as a function
 234 of the fluid dynamic effective radius for the material with density $\rho_{w,(0)} = 88 \text{ kg/m}^3$ and thickness
 235 $h_{(0)} = 40 \text{ mm}$.

236 5. Results and validation

237 The way in which each manufacturing process, presented in section 2, affects the acoustic
 238 performance of the material has been analysed by comparing the normal incidence sound ab-
 239 sorption coefficient α_n , measured on samples of loose hemp fibres at the four different stages of
 240 the process, with identical density $\rho = 88 \text{ kg/m}^3$ and thickness $h = 40 \text{ mm}$. The sound absorp-
 241 tion measurements were performed, as described in section 4, three times for each sample; the
 242 experimental deviation is reported as a shaded area around the average curve of the associated
 243 absorption coefficient. As shown in Figure 3 there is not a relevant difference between the fibres
 244 only carded 01.CAR and the fibres which also went through the alkaline treatment 02.NaOH. In

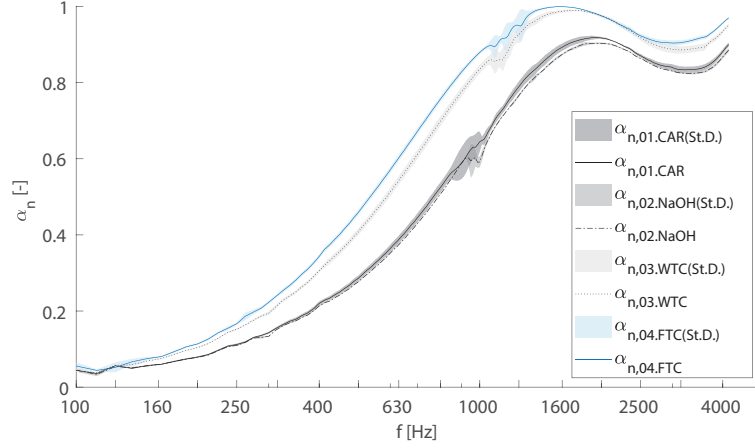


Figure 3: Normal incidence sound absorption coefficient measured on hemp fibres samples, with thickness $h = 40$ mm and density $\rho_w = 88 \text{ kg/m}^3$ at the four different stages of the manufacturing process.

245 fact, even though the sound absorption coefficient associated with the 02.NaOH fibres is slightly
 246 lower than the values related to the carded fibres 01.CAR, these differences are barely notice-
 247 able and the two curves almost match within the entire frequency range. On the other hand, the
 248 wide tooth combing 03.WTC significantly increases the sound absorption of the material. More-
 249 over, the acoustic performance of the hemp fibrous material is further enhanced after the fine
 250 tooth combing treatment 04.FTC, which allows the natural fibrous material to match the normal
 251 incidence sound absorption of traditional synthetic fibres.

252 The characterisation methodology described in the previous section was validated by compar-
 253 ing the physical parameters, computed for a varying compression rate n , with experimental
 254 results. The initial set of material properties computed as a function of the effective radius, derived
 255 from the experimental the air flow resistivity $\sigma_{(0)}$, and function of the normal incidence
 256 sound absorption coefficient $\alpha_{n,(0)}$; both measured on samples of hemp fibres 40 mm thick, with
 257 a density of $\rho_{(0)} = 88 \text{ kg/m}^3$, is provided in Table 2. In order to validate the results, additional
 258 measurements have been made on the hemp fibrous material at each stage of the manufacturing
 259 process. In particular, a total of five different densities ρ_w were experimentally tested within the
 260 range $\rho_{w,i} = 58.7 \div 140.8 \text{ kg/m}^3$, obtaining hmep firus samples with a thickness varying from
 261 $h = 60$ mm to $h = 25$ mm. For each sample the normal incidence absorption coefficient and
 262 the air flow resistivity were experimentally measured as described in section 4. Moreover, the
 263 materials' tortuosity α_∞ was assessed from an ultrasonic experimental method [31], while the
 264 viscous Λ and thermal characteristic lengths Λ' have been evaluated by using well consolidated
 265 inversion techniques [28].

266 In Figure 4 the experimental air flow resistivity, measured on samples of the fibrous mate-
 267 rial, with five different densities, after each processing step, is shown. Results consistent with
 268 the sound absorption coefficients, shown in 3, are found. In fact, for all the investigated densi-
 269 ties the fibres resulting from the process 04.FTC exhibit the higher air flow resistivity, while the

Table 2: Physical parameters of the hemp fibrous materials used as initial data set to characterise the material properties at varying compression rate

	01.CAR	02.NaOH	03.WTC	04.FTC
$h_{(0)}$ [mm]	40	40	40	40
$\rho_{(0)}$ [kg/m ³]	88	88	88	88
$\phi_{(0)}$ [-]	0.93	0.93	0.93	0.93
$\sigma_{(0)}$ [Pas/m ²]	5536.13	4920.17	7883.65	12503.29
$\alpha_{\infty,(0)}$ [-]	1.055	1.055	1.055	1.055
$\Lambda_{(0)}$ [μm]	109.78	115.46	59.61	50.10
$\Lambda'_{(0)}$ [μm]	160.00	170.81	135.56	109.44

270 lowest values are associated with the fibres resulting from the alkaline treatment 02.NaOH; this
271 behaviour is more emphasised as the density increases. A rising high of the air flow resistivity is
272 thus associated with an improvement of the material's absorption coefficient. The experimental
273 air flow resistivity, plotted together with the error bars, which represent the experimental stan-
274 dard deviation, are compared in Figure 4, with the air flow resistivity computed for a varying
275 compression rate $n = 0.5 \div 2$, according to Eq. (17). For each material a good agreement is
276 found between the experimental results and the curve computed using the formulation proposed
277 in this paper $\sigma_{i,(n,A)}$. The results obtained from the linear model proposed by Castagnède for
278 1D compression is also reported as a dotted line $\sigma_{i,(n,1D)}$, in order to demonstrate how it is not
279 suitable for this kind of material, providing inaccurate results, which progressively deviate from
280 the experimental evidence as the density increases.

281 On the other hand, Castagnède equation for 1D compression provides a good approximation
282 of the experimental tortuosity, as shown in Figure 5. Even though, the curve obtained from the
283 linear relationship for 1D compression slightly deviates from the experimental results at the high-
284 est densities, it should be considered that such differences are comparable with the experimental
285 standard deviation, reported as error bars.

286 It was not possible to measure the viscous and the thermal characteristics lengths, these
287 quantities were thus determined, for each material, by using a consolidated inversion technique,
288 minimising the difference between the experimental sound absorption coefficient and the results
289 obtain from the JCA model.

290 However, keeping in mind that at the low frequencies, or for materials with a low density,
291 both the viscous and the thermal characteristics lengths have not a significant influence on the
292 sound absorption coefficient, one soon realises that in these cases the inversion technique would
293 not necessarily provide the best physical solution. In order to provide a sensitivity analysis of
294 the JCA model to these quantities, as a function of the material density, the numerical results
295 were compared with the all values of Λ and Λ' resulting from the minimisation algorithm which
296 guarantee an absorption coefficient within the 3% of error with respect to the experimental value,
297 plotted as a shaded area representing the standard deviation around the best fit results. The
298 standard deviation found in the determination of the characteristic viscous length, as shown in

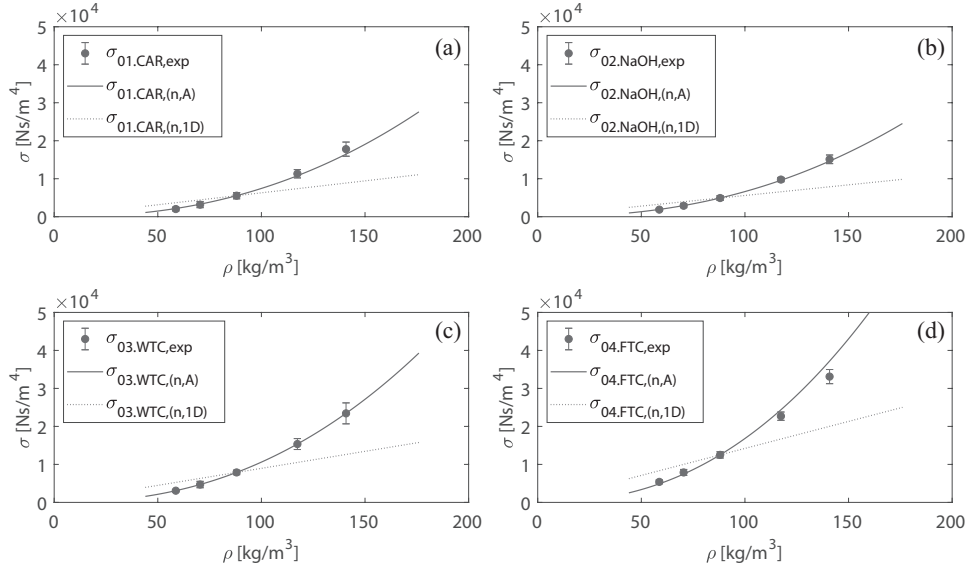


Figure 4: Experimental and estimated air flow resistivity evaluated at each stage of the manufacturing process on samples of various densities at the four manufacturing stages: (a) carding process: 01.CAR; (b) alkaline treatment: 02.NaOH; (c) wide tooth combing: 03.WTC; (d) fine tooth combing: 04.FTC.

299 Figure 6, is very limited for all the four materials, both for high and low densities. However, as
300 the porosity increases the fluid viscosity influence is more significant and the standard deviation
301 further decreases. The numerical curve for a varying compression rate $\Lambda_{(n,1D)}$, given in Figure 6,
302 is in good agreement with the experimental values of the material resulting from the two last
303 manufacturing processes: 03.WTC and 04.FTC; although it significantly deviates from the char-
304 acteristic viscous length evaluated from experimental data for the fibres which underwent only
305 the first two manufacturing treatments: 01.CAR and 02.NaOH. An analogous situation can be
306 drawn comparing the thermal characteristic length derived from the experimental data set and the
307 numerical curve evaluated for a varying compression rate. As it was found for the viscous char-
308 acteristic length, Castagnède equation for 1D compression provide an accurate approximation
309 for the materials obtained from the last two manufacturing process: 03.WTC and 04.FTC, while
310 relevant discrepancies are found for the materials at the first two stages: 01.CAR and 02.NaOH.
311 However, by looking at results obtained from the inversion algorithm, considering all the solu-
312 tions which provide an absorption coefficient within the 3% error, a huge standard deviation is
313 found. This means that the thermal characteristic length does not significantly affect the sound
314 absorption coefficient of materials with high porosity or with rough fibres. The numerical results,
315 even though deviates for the best values solution, represented by black circles, is by far within
316 the shaded area which represents the standard deviation obtained in the minimisation approach.

317 Finally, in order to determined whether the accuracy provided by this approach may guar-
318 antee a good approximation of the material acoustic performance, the experimental sound ab-
319 sorption form normal incidence α_n , measured at each stage of the manufacturing process for five
320 different compression rates, was compared to the results obtained from the JCA model. The
321 physical parameters estimated for a varying compression rate just presented were used as input

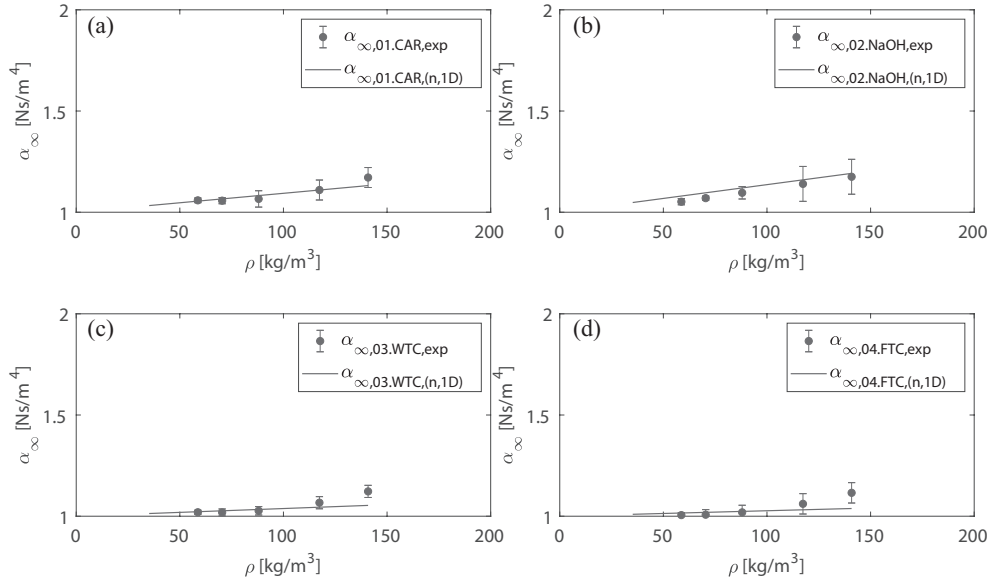


Figure 5: Experimental and estimated tortuosity evaluated on samples of various densities at the four manufacturing stages: (a) carding process: 01.CAR; (b) alkaline treatment: 02.NaOH; (c) wide tooth combing: 03.WTC; (d) fine tooth combing: 04.FTC.

322 data in the model. As shown in Figure 8 a good agreement is found between the numerical re-
 323 sults and the experimental sound absorption for all the four materials at each of the investigated
 324 compression rates. Since the small discrepancies highlighted in some cases between numerical
 325 and experimental curves are comparable with the experimental standard deviation found between
 326 different measurements of the same sample, shown in Figure 3, it can be concluded that the char-
 327 acterisation approach investigated in this study provide an accurate estimation of the physical
 328 parameters required to describe the acoustic performance of hemp fibres materials using the JCA
 329 model.

330 6. Conclusion

331 A study regarding the acoustic performance of hemp fibrous materials and the physical pa-
 332 rameters by which this is affected has been presented. It was analysed how to optimise the
 333 manufacturing process in order to obtain a natural, sustainable and renewable fibrous material,
 334 which can provide an sound absorption coefficient comparable to the one provided by traditional
 335 synthetic fibres. An experimental investigation on hemp-fibres identified the influence of each
 336 stage of the manufacturing process both on the acoustic performance and on the physical charac-
 337 teristics of the fibrous material. It was shown that an alkaline treatment (02.NaOH) performed on
 338 the material after the carding process (01.CAR) does not significantly affect neither its acoustic
 339 performance neither its physical properties, such as the airflow resistivity for example; unless
 340 this is followed by two combing processes, the first one made with a wide tooth comb while the
 341 second with a finer one, which allow to improve the material acoustic performance, by increasing
 342 air flow resistivity and reducing the effective radius of the fibres. From a physical point of view

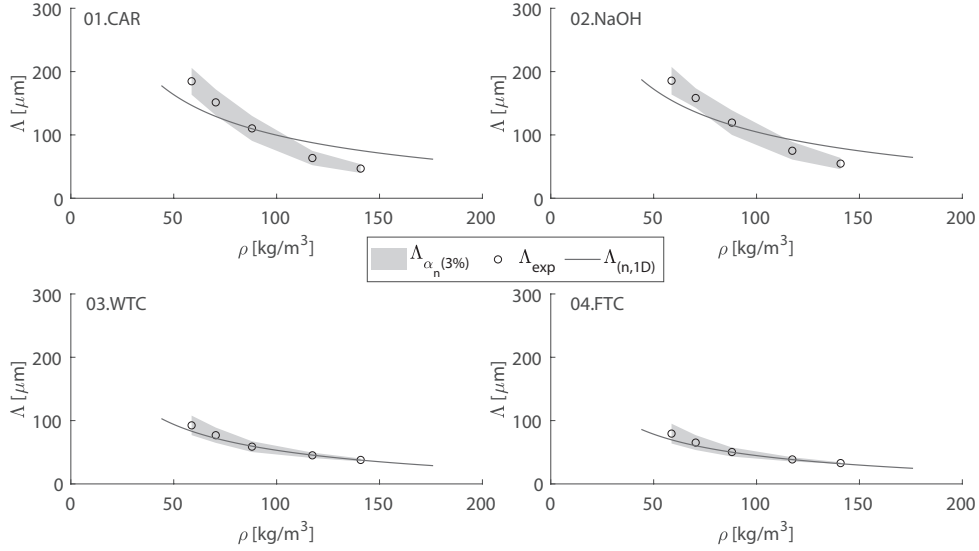


Figure 6: Experimental determined from inversion technique and estimated characteristic viscous length evaluated on samples of various densities at the four manufacturing stages: (a) carding process: 01.CAR; (b) alkaline treatment: 02.NaOH; (c) wide tooth combing: 03.WTC; (d) fine tooth combing: 04.FTC.

343 these processes remove the non-cellulose components extracted by the alkaline treatment. The
 344 physical parameters required to describe the hemp fibres using the JCS equivalent fluid model
 345 were characterised after each manufacturing procedure. Since natural fibres are characterised
 346 by large variability of the diameters distribution, the proposed approach is based on the concept
 347 of effective equivalent fluid-dynamic radius, derived from the experimental air flow resistivity
 348 by using the model developed by Tarnow. Besides, a simplified methodology to investigate the
 349 acoustic performance of hemp fibrous materials, as a function of the material density, was then
 350 proposed, providing an useful tool to compute and compare the sound propagation into the mater-
 351 ial with different degrees of compression. Characterising the hemp fibrous material at the
 352 given density the five physical parameters, used in Johnson-Champoux-Allard model for porous
 353 medium, it was possible to evaluate the properties of the material for a varying compression rate
 354 with good accuracy, by using the simple model developed by Castagnède for mono-axial comp-
 355 ression. However, in order to consider also materials with a high compression rate, i.d. high
 356 density and low porosity, or aspects which are not take into account in this simplified model, such
 357 as the fibres orientation, the 1D linear equation provided to compute the air flow resistivity was
 358 modified by introducing an exponential correction coefficient. Such term was determined from
 359 the experimental airflow resistivity measured on hemp fibres samples at different compression
 360 rates by means of a minimisation algorithm. At each manufacturing stage, all of the investi-
 361 gated parameters numerically evaluated were validated by comparison with the experimental
 362 results, measured on hemp fibres samples with five different densities and thicknesses. More
 363 specifically, the air flow resistivity, the tortuosity and the normal incidence sound absorption
 364 were directly measured, while the viscous and thermal characteristic lengths were determined

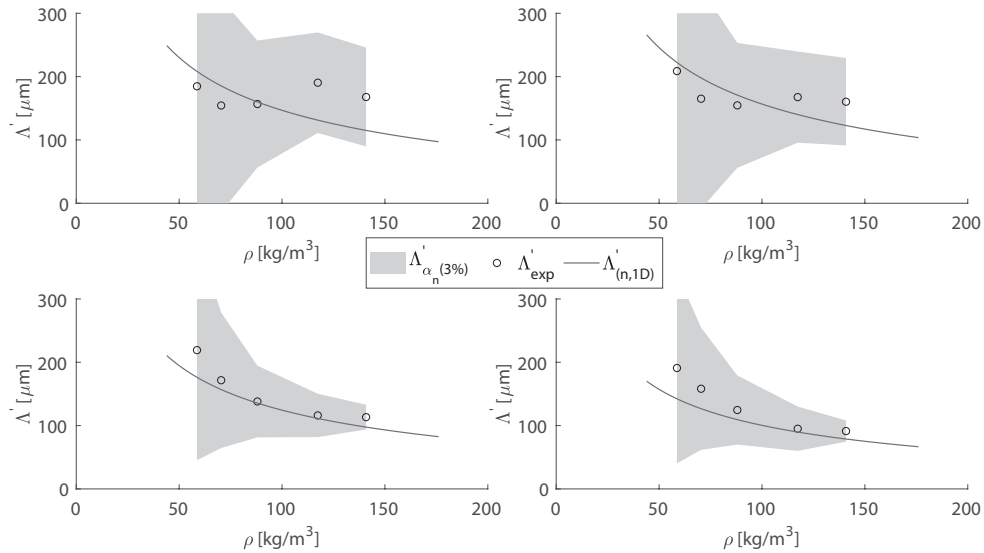


Figure 7: Experimental determined from inversion technique and estimated characteristic thermal length evaluated on samples of various densities at the four manufacturing stages: (a) carding process: 01.CAR; (b) alkaline treatment: 02.NaOH; (c) wide tooth combing: 03.WTC; (d) fine tooth combing: 04.FTC.

365 from the experimental data set using an inversion technique. The validation highlighted a good
 366 agreement between the results obtained from the proposed methodology and the experimental
 367 physical parameters. Due to the simplified and practical nature of the proposed approach some
 368 discrepancies were found, especially at the highest densities. However, the differences found be-
 369 tween the experimental and numerical results were comparable with the experimental standard
 370 deviation obtained from different measurements of the same sample. Moreover, numerically
 371 evaluated parameters used as input data in the Johnson-Champoux-Allard model provided a very
 372 good approximation of the experimental sound absorption coefficient measured at each stage of
 373 the manufacturing process on materials with five densities. The proposed model can be certainly
 374 refined in the follow-up of this project, even though this simplified approach represents a simple
 375 and reliable tool to analyse the acoustic performance of hemp fibrous materials, which was never
 376 investigated before.

377 Acknowledgement

378 We would like to ...

379 References

- 380 [1] S. V. Joshi, L. Drzal, A. Mohanty, S. Arora, Are natural fiber composites environmentally superior to glass fiber
 381 reinforced composites?, *Composites Part A: Applied science and manufacturing* 35 (3) (2004) 371–376.
 382 [2] C. Zhou, S. Q. Shi, Z. Chen, L. Cai, L. Smith, Comparative environmental life cycle assessment of fiber reinforced
 383 cement panel between kenaf and glass fibers, *Journal of Cleaner Production* 200 (2018) 196–204.

- 384 [3] C. Ingrao, A. L. Giudice, J. Bacenetti, C. Tricase, G. Dotelli, M. Fiala, V. Siracusa, C. Mbohwa, Energy and envi-
 385 ronmental assessment of industrial hemp for building applications: A review, *Renewable and Sustainable Energy*
 386 *Reviews* 51 (2015) 29–42.
- 387 [4] F. Iucolano, B. Liguori, P. Aprea, D. Caputo, Thermo-mechanical behaviour of hemp fibers-reinforced gypsum
 388 plasters, *Construction and Building Materials* 185 (2018) 256–263.
- 389 [5] F. Asdrubali, S. Schiavoni, K. Horoshenkov, A review of sustainable materials for acoustic applications, *Building*
 390 *Acoustics* 19 (4) (2012) 283–311.
- 391 [6] F. Asdrubali, F. D’Alessandro, S. Schiavoni, A review of unconventional sustainable building insulation materials,
 392 *Sustainable Materials and Technologies* 4 (2015) 1–17.
- 393 [7] A. Santoni, P. Bonfiglio, F. Mollica, P. Fausti, F. Pompoli, V. Mazzanti, Vibro-acoustic optimisation of wood plastic
 394 composite systems, *Construction and Building Materials* 174 (2018) 730–740.
- 395 [8] M. Delany, E. Bazley, Acoustical properties of fibrous absorbent materials, *Applied acoustics* 3 (2) (1970) 105–116.
- 396 [9] Y. Miki, Acoustical properties of porous materials-modifications of delany-bazley models, *Journal of the Acoustical*
 397 *Society of Japan (E)* 11 (1) (1990) 19–24.
- 398 [10] D. L. Johnson, J. Koplik, R. Dashen, Theory of dynamic permeability and tortuosity in fluid-saturated porous
 399 media, *Journal of fluid mechanics* 176 (1987) 379–402.
- 400 [11] Y. Champoux, J.-F. Allard, Dynamic tortuosity and bulk modulus in air-saturated porous media, *Journal of applied*
 401 *physics* 70 (4) (1991) 1975–1979.
- 402 [12] D. Lafarge, P. Lemarinier, J. F. Allard, V. Tarnow, Dynamic compressibility of air in porous structures at audible
 403 frequencies, *The Journal of the Acoustical Society of America* 102 (4) (1997) 1995–2006.
- 404 [13] M. Garai, F. Pompoli, A simple empirical model of polyester fibre materials for acoustical applications, *Applied*
 405 *Acoustics* 66 (12) (2005) 1383–1398.
- 406 [14] U. Berardi, G. Iannace, Acoustic characterization of natural fibers for sound absorption applications, *Building and*
 407 *Environment* 94 (2015) 840–852.
- 408 [15] C. Piégay, P. Gle, E. Gourdon, E. Gourlay, S. Marceau, Acoustical model of vegetal wools including two types of
 409 fibers, *Applied Acoustics* 129 (2018) 36–46.
- 410 [16] H. Mamtaz, M. H. Fouladi, M. Al-Atabi, S. Narayana Namasivayam, Acoustic absorption of natural fiber compos-
 411 ites, *Journal of Engineering* 2016.
- 412 [17] Z. Lim, A. Putra, M. Nor, M. Yaakob, Sound absorption performance of natural kenaf fibres, *Applied Acoustics*
 413 130 (2018) 107–114.
- 414 [18] V. Tarnow, Measurement of sound propagation in glass wool, *The Journal of the Acoustical Society of America*
 415 97 (4) (1995) 2272–2281.
- 416 [19] B. Castagnede, A. Aknine, B. Brouard, V. Tarnow, Effects of compression on the sound absorption of fibrous
 417 materials, *Applied Acoustics* 61 (2) (2000) 173–182.
- 418 [20] M. Horne, Bast fibres: hemp cultivation and production, in: *Handbook of Natural Fibres: Types, Properties and*
 419 *Factors Affecting Breeding and Cultivation*, Elsevier, 2012, pp. 114–145.
- 420 [21] L. Y. Mwaikambo, M. P. Ansell, Chemical modification of hemp, sisal, jute, and kapok fibers by alkalization,
 421 *Journal of applied polymer science* 84 (12) (2002) 2222–2234.
- 422 [22] J. Zhang, H. Zhang, J. Zhang, Effect of alkali treatment on the quality of hemp fiber., *Journal of Engineered Fabrics*
 423 *& Fibers (JEFF)* 9 (2).
- 424 [23] H. T. Luu, R. Panneton, C. Perrot, Effective fiber diameter for modeling the acoustic properties of polydisperse
 425 fiber networks, *The Journal of the Acoustical Society of America* 141 (2) (2017) EL96–EL101.
- 426 [24] V. Tarnow, Airflow resistivity of models of fibrous acoustic materials, *The Journal of the Acoustical Society of*
 427 *America* 100 (6) (1996) 3706–3713.
- 428 [25] EN 29053 – Acoustics - Materials for acoustical applications - Determination of airflow resistance, Standard,
 429 European Committee for Standardisation, Brussels, Belgium (1993).
- 430 [26] ISO 10534-2 – Acoustics – Determination of sound absorption coefficient and impedance in impedance tubes –
 431 Part 2: Transfer-function method., Standard, International Organization for Standardization, Geneva, CH (1998).
- 432 [27] H. T. Luu, C. Perrot, R. Panneton, Influence of porosity, fiber radius and fiber orientation on the transport and
 433 acoustic properties of random fiber structures, *Acta Acustica united with Acustica* 103 (6) (2017) 1050–1063.
- 434 [28] P. Bonfiglio, F. Pompoli, Inversion problems for determining physical parameters of porous materials: Overview
 435 and comparison between different methods, *Acta Acustica united with Acustica* 99 (3) (2013) 341–351.
- 436 [29] B. Campolina, N. Dauchez, N. Atalla, O. Doutres, Effect of porous material compression on the sound transmission
 437 of a covered single leaf panel, *Applied Acoustics* 73 (8) (2012) 791–797.
- 438 [30] L. Lei, N. Dauchez, J. Chazot, Prediction of the six parameters of an equivalent fluid model for thermocompressed
 439 glass wools and melamine foam, *Applied Acoustics* 139 (2018) 44–56.
- 440 [31] P. Bonfiglio, F. Pompoli, et al., Frequency dependent tortuosity measurement by means of ultrasonic tests, in:
 441 *Proceeding of the 14th International Congress on Sound and Vibration*, Vol. 14, ICSV, Cairns, Australia, 2007, pp.
 442 1–6.

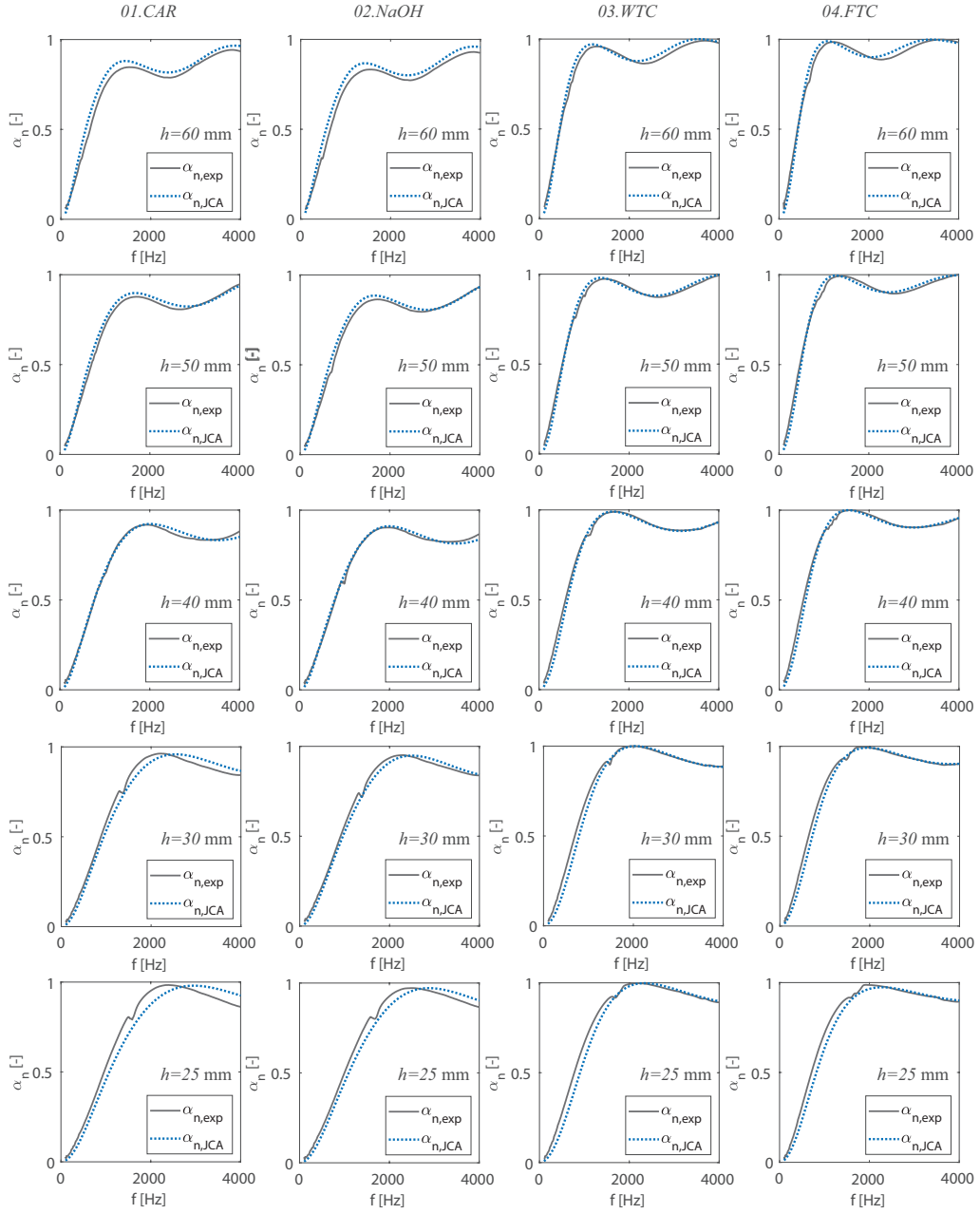


Figure 8: Comparison between numerical and experimental normal incidence sound absorption coefficient of the hemp fibrous material at each stage of the manufacturing process, for different compression rate.